AHS 70th Annual Forum
Montreal, Quebec, Canada
May 20-22, 2014

Operating Strategies and Design Recommendations for Mitigating Local Damage Effects in Offshore Turbine Blades

Phillip W. Richards
phillip@gatech.edu
Graduate Research Assistant
Daniel Guggenheim School of Aerospace Engineering
Atlanta, Georgia, USA

D. Todd Griffith
dgriffi@sandia.gov
Principal Member of the Technical Staff
Sandia National Laboratories
Albuquerque, New Mexico, USA

Dewey H. Hodges
dhodges@gatech.edu
Professor
Daniel Guggenheim School of Aerospace Engineering
Atlanta, Georgia, USA

ABSTRACT

Two major barriers to widespread US acceptance of offshore wind energy is reliability of rotor blades and the difficulty to access for inspection and maintenance. This work presents operation and design strategies aimed to increase blade reliability and maximize power production. Operating strategies that prolong blade life while optimizing energy output allow for smarter maintenance planning and lower maintenance costs. Offshore plants require significant balance of station costs associated with each turbine, leading to large rotor diameters to capture the most energy per turbine. Rotor diameters have already approached 130 m, so this work extends that trend to 100 m blade (205 m diameter) designs. A combined aero/structural optimization process was used to produce new 100 m blade designs. A high-fidelity analysis method is presented to assess the local damage effects of a common damage type. The operation and design strategies are then compared for their effect to mitigate the local damage effects.

Sandia National Laboratories is a multi-program laboratory managed and operated by Sandia Corporation, a wholly owned subsidiary of Lockheed Martin Corporation, for the U.S. Department of Energy's National Nuclear Security Administration under contract DE-AC04-94AL85000.

INTRODUCTION

Offshore wind power production is an attractive clean energy option, but there are several challenges to overcome if offshore wind is to be a viable energy source. Offshore plants require significant balance of station costs associated with each turbine, leading to large rotor diameters to capture the most energy per turbine. To investigate issues that arise with large blades, Sandia National Laboratories produced an all-glass design for a 100 m blade (Ref. 1) and a design utilizing carbon fiber (Ref. 2). An overview of the 100 m blade design project is given by Griffith et al. (Ref. 3). More conventional large turbine designs are in the neighborhood of 125 m diameter (63 m blade length), which is exemplified by the NREL 5 MW baseline turbine (Ref. 4).

The distance from shore creates significant operations and maintenance issues, sometimes leading to long periods between maintenance or inspection opportunities. The Structural Health and Prognostic Management (SHPM) project at Sandia National Laboratories attempts to address these issues by proposing a structural health and prognostic management system (Ref. 5). The overall flow chart for the SHPM project is shown below in Fig. 1. So far, it is has successfully shown that blade sensor measurements have the capability to estimate the size, nature, and location of blade damage (Refs. 6,7). Simple fatigue considerations have identified the potential to derate the damaged turbine and significantly increase its fatigue life. Initial operating and maintenance cost models have been developed to predict the reduction in operating and maintenance costs that can be achieved using a prognostic control strategy, based on probabilities of progression from one damage state to another (Ref. 6). Here derating defers to altering the speed/pitch controller to limit the

Presented at the AHS 70th Annual Forum, Montréal, Québec, Canada, May 20 – 22, 2014.

power production to a level lower than the normal rating of the turbine. This work concerns the "local" effects of damage, in terms of the opening/closing behavior of discrete damage features, early onset of buckling due to disbonded surfaces, etc. High-fidelity analysis techniques such as finite element analysis (FEM) should be used to evaluate these local effects of damage in order to characterize and quantify the risk of operating at a derated level when damage is known to exist. Understanding the local behavior of common damage types will then lead to development of operating and design strategies for more reliable offshore wind turbine blades.

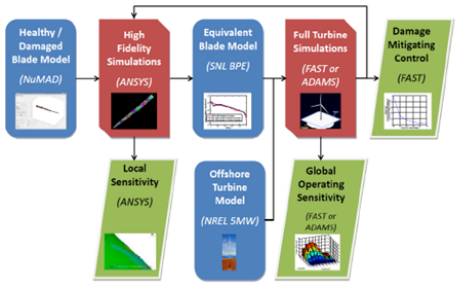

Fig. 1: The SHPM multi-scale damage modeling and simulation methodology.

BACKGROUND

A general cost-benefit analysis of offshore wind energy is presented by Snyder and Kaiser (Ref. 8). This analysis identifies the relative cost and risk of offshore turbines (compared with onshore) as a main barrier for acceptance of offshore wind, and highlights the larger percentage of operational and maintenance costs of the total offshore cost of energy (compared with onshore). A major goal of the SHPM project is to present operational and control strategies for offshore wind farms that will minimize the total cost of energy, by avoiding blade damage or mitigating blade damage growth with smart loads management.

The purpose of the smart loads management system is to (a) avoid a catastrophic failure through advance warning (b) plan cheaper maintenance and (c) increase energy capture by avoiding shutdown. The resulting strategies will consist of decisions to shut down, operate the turbine normally, or operate potentially damaged turbines in a safe way. The recommendation to operate damaged turbines must justify the risk of further damage to the turbine based on the local sensitivity analysis results and the potential to increase the annual energy production (AEP). where inspection and maintenance can be difficult. An effective prognostic control strategy will therefore reduce the total cost of energy by reducing O&M costs as well as increasing power production for offshore wind farms.

Operation and Maintenance Strategies

Decisions of how to operate a turbine should be made in conjunction with an inspection and maintenance scheduling strategy. An overview of maintenance management is given by Frangopol et al. (Ref. 9). Rangel-Ramirez and Sorensen (Ref. 10) applied a risk-based inspection strategy from offshore oil industry to offshore wind farms, showing that operational decisions regarding inspections should consider turbulent wake effects of the farm as a whole. Zhang et al. (Ref. 11) use a wake-loss model and historical data to define an inspection model that accounts for the wake of each turbine. This inspection model would use weather reports when available and historical data when necessary to make up-to-date decisions. This way wind turbines heavily affected by the wake(s) of one or more other turbines or whose wake affects other turbines would be shut down in favor of turbines operating optimally. This model in particular would be an ideal starting point for an operational strategy that includes damage tolerance considerations. A damaged turbine that is forecasted to be partially within the wake of another, for example, would likely remain shut down, while a damaged turbine that is forecasted to be within a clear inflow would then operate under a prognostic control system. Wenjin et al. (Ref. 12) proposed a predictive maintenance strategy based on modeling the blade deterioration with Monte Carlo simulations. This is again similar to the proposed operations strategy, except that the damage detection efforts of the SHPM project are intended to augment or replace blade deterioration models (Refs. 6, 7). Also, high-fidelity damage tolerance analysis will be used to justify the risk of continued operation.

Control System Considerations

Under "normal" operation, a wind farm is operated to maximize power production. Modern wind turbines of 5 MW or larger are typically controlled in yaw, pitch, and rotor angular speed to optimize their power production capability. The yaw control is used to align the rotor with the wind direction, while pitch and speed controls are primarily used to control aerodynamic loads and generator performance. The rotational speed of the turbine controlled via torque control of the generator. The pitch and speed controls of each turbine can either be used individually to maximize the power output of each individual turbine, or in a collective sense to maximize the power output of the wind farm as a whole (Refs. 13–15). For this research, the NREL 5 MW baseline design (Ref. 4) will be considered as a representative offshore turbine design with yaw, pitch, and rotor speed controls.

Under "damaged" operation, the control strategies will be used to produce power production while alleviating loads on damaged blades. Bossanyi has studied the

blade load reduction problem extensively (Ref. 16). One example of individual blade control design using sliding-mode control is given by Xiao et al. (Ref. 17). Pitch control is often used to mitigate vibrations of offshore platforms, including the use of individual blade pitch control (Refs. 18–22), and structural control methods (Ref. 23). These vibrations create fatigue damage of the foundation (Ref. 24), so are often the focus of offshore wind turbine control design efforts. Accurate platform fatigue analysis requires nonlinear modeling of the wave conditions (Ref. 25). In general, the structural health monitoring systems should be integrated with the operation and controls of the wind turbine as demonstrated by Frost et al. (Ref. 26). A good prognostic control strategy would address all of these issues in addition to possible blade damage, but these considerations are beyond the scope of the current research. It is enough to say that pitch control techniques have been shown to have a wide variety of applications to blade-load reduction.

Damage Tolerance Analysis

The study of damage tolerance is a field in and of itself, with the damage tolerance of composites being currently quite active. A good review of the subject is given by Fan et al. (Ref. 27). Damage tolerance predictions may be divided into two categories: stress-based approaches and energy-based approaches. Stress-based approaches are quite useful for isotropic, ductile materials, but the anisotropic, brittle nature of composites leads to singular stress fields and damage mechanisms that are very different from those in metallic materials. Despite this, these techniques still give a reasonable prediction of fatigue life and therefore are useful for preliminary and conceptual design. The onset of damage is predicted using an S-N curve and Miner's rule; several recent Sandia reports cover these analysis techniques quite thoroughly (Refs. 28–30).

Energy-based methods are often preferred for prediction of damage initiation and growth in composites. These energy-based methods involve calculation of the Strain Energy Release Rate (SERR), which is an estimate of the strain energy released when a crack opens from length a to $a+da$ and is commonly referred to by the symbol G. Regardless of the material, the field of damage tolerance typically recognizes three distinct modes of crack propagation, referred to as Mode I, II, and III. Therefore, the energy-based prediction method will typically provide three values of G for each mode, denoted G_I, G_{II}, and G_{III}. Fracture is assumed to occur with energy-based methods when some combination of the G values for each mode reaches a material-dependent parameter known as the fracture toughness G_c. The way in which the G values are combined depends on mode-mixity models, which are typically extracted from experimental data.

One popular energy-based method is the Virtual Crack Closure Technique (VCCT), which is reviewed by Krueger (Ref. 31). The VCCT essentially operates on the assumption that as the crack opens from size a to $a+da$, the internal forces at the crack tip do not change significantly. When attempting to close a crack from length $a+da$ to length a, the energy required will be the opened displacements multiplied by the internal forces that resist the closure. The main assumption of the VCCT allows the forces at the crack tip to be used in this calculation. Therefore, the resulting formulas for the SERR in modes I, II, and III are, respectively,

$$\begin{aligned} G_I &= \tfrac{1}{2\Delta a} F_y (u_y - \bar{u}_y) \\ G_{II} &= \tfrac{1}{2\Delta a} F_z (u_z - \bar{u}_z) \\ G_{III} &= \tfrac{1}{2\Delta a} F_x (u_x - \bar{u}_x) \end{aligned} \tag{1}$$

where u_i are the displacements of the upper surface and $\bar{u}_i$ are the displacements of the lower surface. Here, y refers to the direction perpendicular to the line of the crack in the "opening" direction, z refers to the direction along the line of the crack, and x refers to the direction perpendicular to the opening direction and the line of the crack. Neglecting any pretwist of the blade or displacements, these coincide with the coordinate definitions of the NuMAD model. This method has been recently applied to the problem of trailing edge disbonds by Eder et al. (Ref. 32) to predict damage onset location and assess the effect of loading directions on the blade. They concluded that Mode III is the governing Mode of fracture for this type of damage and that flapwise shear and torsion are the most important load cases.

Design Strategies for Damage Tolerance

The design of damage tolerant composite structures typically involves avoiding delamination by introducing "dispersion" into laminates and analyzing the adhesion of various types of bonded joints. The concept of dispersion is described by Lopes et al. (Ref. 33) and involves avoiding placing adjacent layers at the same layup angle so that cracks will be arrested at the interface between layers. Damage tolerance is also of primary concern in the design of adhesive joints, as illustrated by Kim, Kwon, and Keune (Ref. 34) in their study of adhesively bonded fuselage skins.

Damage tolerant design efforts for wind turbine blades need to consider the loading environment as well as common damage types. For example, Schaumann et al. (Ref. 35) use a time domain approach to consider fatigue

loading from wind and waves in the design process of offshore platform support structures. Wetzel (Ref. 36) showed that spar caps embedded in the skin are less susceptible to spar bond failures, another example of damage tolerant structural design. Skin buckling is a primary design factor in large rotor blade design. Disbonded surfaces typically worsen the skin buckling performance, whether due to changing the boundary conditions (in the case of a trailing edge disbond) or increasing the effective panel size (in the case of a spar/skin disbond). Therefore, a blade with a higher skin buckling capacity can be thought of as more damage tolerant in general. Concerning disbonding of adhesively bonded fuselage skins Kim, Kwon, and Keune (Ref. 34) state "the driving force for disbond growth following buckling initiation is the postbuckling deformations," so the panel buckling performance can be tied to damage tolerance for some damage types.

APPROACH AND RESULTS

This research will take a multi-scale analysis approach to the problem. The Sandia National Laboratories Numerical Modeling and Design (NuMAD) tool is an open-source tool for analyzing realistic composite wind turbine blades (Ref. 37). This tool has the capability of transforming a traditional beam and section definition of a wind turbine model into a high-fidelity ANSYS shell model. Since this capability is readily available to interested academic and industry parties and it produces a high-fidelity model of the blade as a whole, this shell modeling capability was utilized for this study as the "global" analysis. The shell model does not have a sufficiently refined mesh near the trailing edge, which is the area of interest of this research, so the global analysis needs to be supplemented with a "local" analysis as well. To demonstrate the method, only the "global" analyses are shown here, but the refined "local" analysis results may be available for the presentation. The criticality of trailing edge disbonds with respect to damage location was examined for both the NREL 5 MW (63 m radius) and the SNL 100-02 (102.5 m radius) blade designs. Two simple derating strategies were explored using beam analysis tools such as WT_Perf and FAST/AeroDyn as well as using the "global" shell model to determine the capability of the strategy to mitigate local damage effects. Then, a combined aero/structural optimization was used to produce several new design candidates for the 100 m blade. These candidates are compared in terms of conventional measures such as geometry, AEP, blade weight, and stress-based fatigue damage as well as in terms of the damage tolerance of each design in the case of a trailing edge disbond.

ANSYS Analysis of Strain Energy Release Rates (SERRs)

The global NuMAD shell model was modified by removing the connectivity of elements adjacent to the trailing edge, adding coincident nodes along the trailing edge, and reconnecting the upper elements to the new coincident nodes. Then, COMBIN elements, which are essentially nonlinear springs, were used to connect the coincident nodes. The stiffness behavior of the COMBIN elements was modified to have zero stiffnesses in the "X" (chordwise) and "Z" (spanwise) directions and in the positive "Y" (flapwise) directions, but a very high stiffness in the negative "Y" direction. This approach was verified to model the opening/closing behavior of the disbonds. The loading at rated windspeed during normal or derated operation was calculated using WT_Perf, which is a blade-element/momentum theory solver for wind turbines provided by the National Renewable Energy Laboratory (NREL). The distributed loading from the WT_Perf model was then applied to the ANSYS model via the application of point loads at each external node in the ANSYS model. The value of the point loads was obtained by performing a least-squares regression to determine a value of forces at each node to produce the desired distributed forces and twisting moments. The capability to map distributed loads to the ANSYS model is included in the NuMAD functionality (Ref. 38).

The SERR was calculated from the "global" model by using the resulting nodal forces at the crack tip and the opened displacements of the nodes just within the crack tip. At this time, the "global" results are not fully trusted to be numerically accurate to the actual SERRs within the propagation, but it is assumed that these results are sufficient for demonstrating general trends. The values of G_I, G_{II}, and G_{III} were calculated for a 2 m disbond initiating at various points along the inner portion of the blade and are shown in Figs. 2 – 4. In these figures and onward, "Inboard" refers to the inboard crack tip and "Outboard" refers to the outboard crack tip. These show that for G_I and G_{III}, there seem to be critical areas for each blade. For the NREL 5 MW blade, the areas of 6 m and 8 m were chosen as areas of interest for G_{III} and G_I, respectively.

Potential SHPM Operation and Control Strategies

The simplest example of a load-reducing, pitch-control method is to utilize the available pitch-control system to control blade RPM and pitch to limit the power production to a lower level (Refs. 6, 26). For this research, the derating was accomplished by holding the RPM constant above the windspeed when the power production exceeds its derated level at a 0° pitch setting, and then using the

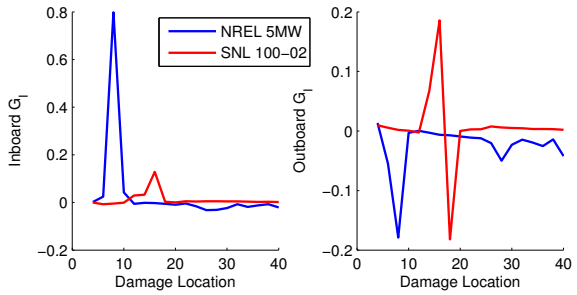

Fig. 2: Damage criticality trends for G_I for the NREL 5 MW and SNL 100-02 blade at the rated windspeed.

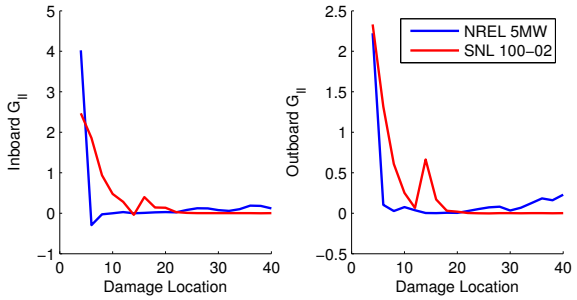

Fig. 3: Damage criticality trends for G_{II} for the NREL 5 MW and SNL 100-02 blade at the rated windspeed.

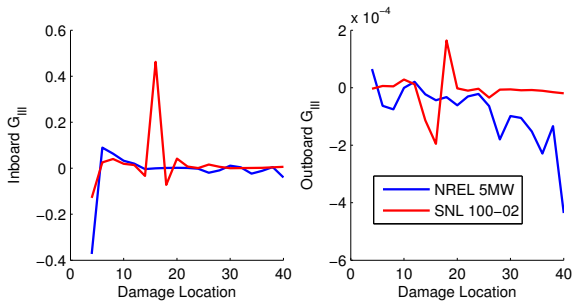

Fig. 4: Damage criticality trends for G_{III} for the NREL 5 MW and SNL 100-02 blade at the rated windspeed.

pitch controller to maintain the power production as the windspeed increases. For the NREL 5 MW baseline turbine, a 50% derating strategy, and a Rayleigh wind profile with average windspeed of 10 m/s, the AEP is reduced from $\approx 2.5 \times 10^7$ kWh to $\approx 1.5 \times 10^7$ kWh. The advantage to using a simple "derating" method is that it would only involve a change in the software of currently operating offshore turbine control systems, and therefore could be easily retrofitted into pre-existing designs.

Two different ways to reduce service bending moments by derating were evaluated: limiting the value of the bending moment or thrust without limiting the power rating (derating strategy "A"), or limiting the power rating (derating strategy "B"). Figure 5 shows an example of the two derating strategies for the case of limiting the bending moment to 50% of its maximum value. The NREL 5 MW baseline design is used for the operations and control strategy evaluations as a representative of "current" offshore blade technology. The AEP of the NREL 5 MW baseline turbine for a possible Alaska location with a one-month shutdown, using wind data from Pryor et al. (Ref. 39), is then shown in Table 1. The location was chosen as a realistic representative site with an average windspeed of ≈ 10 m/s. The additional revenue for operating at a derated level for the 12$^{\text{th}}$ month instead of shutting down is also given in Table 1. Figure 6 shows the windspeed monthly variation as measured at a Baltic offshore site which has an approximate average windspeed of 11 m/s, and Table 2 shows how the additional revenue could vary.

To evaluate the realism of such a derating strategy, derating strategy "B" was analyzed using a FAST/AeroDyn windspeed sweep and compared to the baseline performance. Figures 7 – 8 show the speed controller and root bending moment predictions from the two analyses. These figures show the FAST/AeroDyn implementation varies slightly from intended, as the rotor speed was not intended to change. However, the power prediction and pitch controller performance were similar to predicted and the strategy successfully lowers the maximum bending moment by around 25%. The difference between these results and WT_Perf predicted reduction of 50% is due to a slight difference in the way the two loads are defined. Therefore, the WT_Perf loads were used in this report to calculate the SERRs for the normal and derated case.

The effect of these strategies in reducing the SERRs was also evaluated. The criticality analysis in Section identified the 6 m and 8 m locations as areas of interest. Therefore, these areas were analyzed for G_I and G_{III} under the derating strategies "A" and "B." Figure 9 and 10 show how the SERRs at the areas of interest change with windspeed under normal and derated operation. These figures show a behavior similar to the thrust/moment vs. windspeed behavior (Fig. 5). The SERRs were then summed using a probability-weighted sum (similar to the way AEP is calculated), producing a weighted average SERR for each operating strategy. A Rayleigh windspeed distribution with an average windspeed of 10 m/s was used. This allowed calculation of an effective reduction in SERR due to the derating, which is shown for the 8 m disbond location in Table 3. These effective reductions could be thought of an effective decrease in damage growth rate while operating under the derated strategy. When results are refined with multi-scale analysis techniques and a growth law is applied, then effective reduction in damage growth rate can be predicted. These predictions will then be used to design a more comprehensive operations strategy to maximize power output while also maintaining blade reliability.

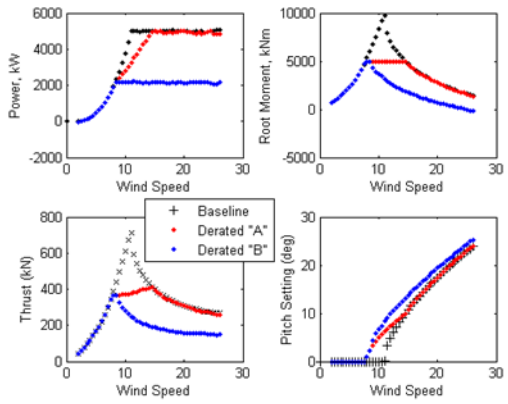

Fig. 5: Power production, root bending moment, rotor thrust predictions for two derating strategies "A" and "B" and derating level of 50%. The derating strategies are achieved by modifying the pitch control settings as shown in lower-right.

Table 1: Annual revenue and revenue increases (using 5 ¢/kWh) for operating at derated level for 1 month instead of shutdown.

	Alaska Site (9.9 m/s)
Annual Revenue	$1,210,000
Derating Level	Additional Revenue
75% (A)	+$108,000 (+8.9%)
75% (B)	+$81,600 (+6.8%)
50% (A)	+$96,000 (+8.0%)
50% (B)	+$64,000 (+5.3%)
25% (A)	+$60,400 (+5.0%)
25% (B)	+$22,900 (+1.9%)

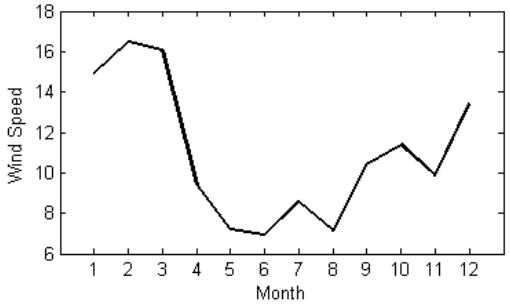

Fig. 6: Monthly variation in windspeed for a Baltic offshore site with a windspeed average of 11 m/s (Ref. 40).

Design Strategies for Damage Tolerance

The Sandia 100 m carbon blade design is used as a baseline for the reliable blade design process, as it represents a trend in future blade designs. A significant issue in the 100 m blade design precess was panel buckling, and these buckling issues can worsen in the presence of damage. The buckling performance can be improved by reducing the skin panel size, which provides an incentive for low solidity blade designs. The solidity of the blade can be decreased by increasing the operating tip speed ratio and implementing higher lift airfoils. So-called flatback (FB) airfoils have high-lift properties, and the flat trailing edge provides an ideal location for trailing edge reinforcement. Trailing edge disbonding is a commonly encountered damage type and such reinforcement would improve the tolerance of blade designs to this type of damage. So that "apples-to-apples" comparisons can be made between the new airfoils and the baseline airfoils, an optimized design was also produced with the baseline set of airfoils as well. The optimization process resulted in a Pareto front of candidates, which were then analyzed for their performance in terms of damage tolerance. The process indicated that weight reduction and annual energy output (AEP) increases can be achieved by increasing the optimum (design) tip speed ratio and rotor solidity, but that damage tolerance considerations may place a limit on how high the design tip speed ratio should be raised. This is demonstrated by comparing two optimized designs with the DU series airfoils with two optimized designs with FB airfoils.

Table 2: Variations due to monthly windspeed variation in possible revenue increases (using 5 c/kWh), when derating for 1 month instead of shutdown.

Level	Calm (7 m/s)	Windy (16.5 m/s)
75% (A)	+$63,800 (+4.9%)	+$140,000 (+10.7%)
75% (B)	+$53,400 (+4.1%)	+$99,100 (+7.6%)
50% (A)	+$55,800 (+4.3%)	+$131,000 (+10.0%)
50% (B)	+$44,500 (+3.4%)	+$73,800 (+5.6%)
25% (A)	+$35,300 (+2.7%)	+$96,800 (+7.4%)
25% (B)	+$19,200 (+1.5%)	+$23,900 (+1.8%)

Table 3: Reduction in averaged SERRs for 8 m disbond location under derated operation, weighted by a Rayleigh wind distribution with average windspeed of 10 m/s.

Derating Strategy	A	B
Reduction in G_I	35%	70%
Reduction in G_{II}	33%	70%
Reduction in G_{III}	47%	63%

Combined Aero/Structural Optimization A multi-objective optimization process was conducted using the optimization tool HARP_Opt, integrated with Sandia National Laboratories NuMAD toolbox and an open source code for composite wind turbine blade structural analysis, CoBlade (Refs. 41–43). The MATLAB Genetic Algorithm is used for the optimization process, with the objective functions being AEP and blade mass. After an optimization run, a Pareto front of candidates is produced. The selection of one particular candidate along the Pareto

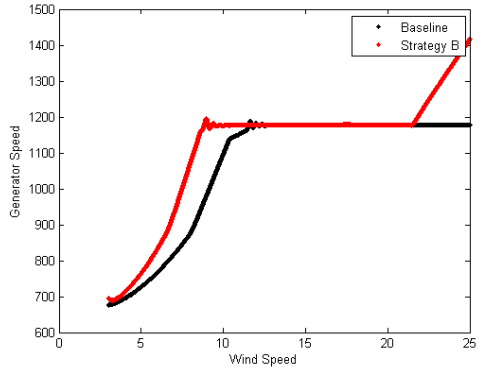

Fig. 7: Rotor speed controller performance for NREL 5 MW baseline turbine for normal and derated operation.

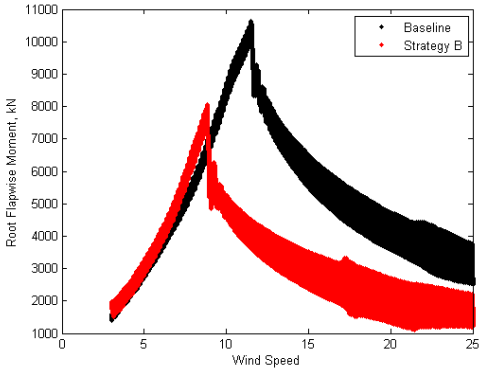

Fig. 8: Flapwise bending moment predictions for NREL 5 MW baseline turbine for normal and derated operation.

front should be based on economic decisions, so the increased costs associated with blade weight, including material and manufacturing costs, should be weighed against the potential for increased power output. However, such a detailed economic model is often based on prior experience and in this case difficult to apply. Therefore, the two candidates on the Pareto front were investigated in terms of blade weight, AEP, and damage tolerance: one candidate with the same AEP as the baseline, and another at an increased level of AEP. Therefore four candidates in total resulted from the optimization process, two with DU airfoils and two with flat-back (FB) airfoils. The candidates with the same AEP as the baseline will be referred to as DU #1 and FB #1, and the increased AEP candidates are DU #2 and FB#2.

The damage tolerance analyses included a stress-based fatigue analysis based on the S-N law and Miner's rule. Representative material properties for the carbon fiber, unidirectional glass, and bidirectional skin material were used in the S-N analysis. The number of cycles and loading magnitudes are obtained from FAST/AeroDyn

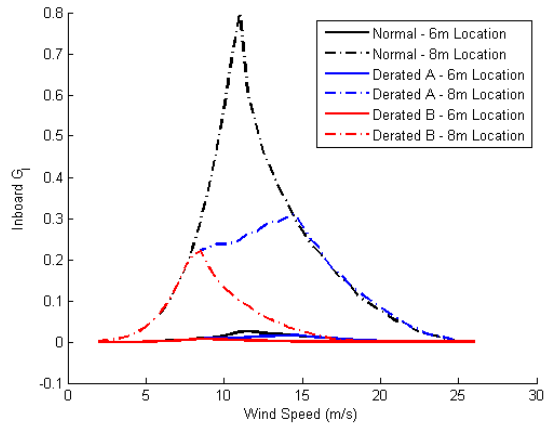

Fig. 9: G_I with respect to windspeed for NREL 5 MW turbine in normal/derated operation.

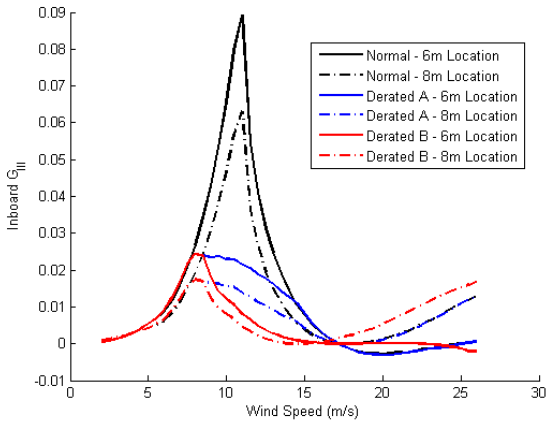

Fig. 10: G_{III} with respect to windspeed for NREL 5 MW turbine in normal/derated operation.

analysis of turbulent operation at each windspeed. Then, Miner's rule was used to sum the fatigue damage at each windspeed using the design windspeed profile, and the fatigue life was calculated. An ANSYS model of each design was created and used to calculate the buckling capacity at the maximum service loading condition. This ANSYS model was then used to perform a damage criticality analysis (SERRs) of each design.

An overview of each design including the analysis results is given in Tables 4 – 5. The twist, chord, and spar layers distributions of each design are summarized in Figs. 11 – 12. Figures 13 – 15 show some details about the aerodynamic performance of the different designs compared with the baseline. The optimized designs each feature an increased optimal tip speed ratio (TSR), which is demonstrated in Fig. 15 and results in a shift of the power production to lower windspeeds. These results highlight the tradeoff between design TSR, blade solidity, blade weight and AEP. While the "damage tolerance"

of the blade design in terms of the fatigue life calculation decreases with increasing TSR (decreasing solidity), the buckling margin increases as the solidity decreases. Therefore, the "damage tolerance" criterion would seem to suggest a moderate increase in the design TSR with respect to the SNL 100-02 design. The fatigue life of the FB airfoils was generally improved with respect to the DU airfoils, especially considering that a lower number of spar layers are used in the FB designs.

The damage criticality analysis was performed for each design for a trailing edge disbond length of 2 m. The resulting SERR values are given in Figs. 21 – 26. The optimized design DU #1, which had the same AEP and airfoil selection as the baseline design, but a greatly increased design TSR and reduced blade solidity, was found to have a higher peak in G_I, but generally decreased values in G_{II} and G_{III}. The DU #2 design, which has a moderately increased TSR, generally has lower SERR values. This suggests that the DU #2 design is the most damage tolerant design with respect to this damage type (TE disbond). The FB designs have lower G_{III} values, but G_I and G_{II} are higher for most of the damage onset locations. The SERR values for the FB designs are lower than the DU designs over the 10 – 20 m span location, which suggests that the FB airfoils could be used over this location to improve the damage tolerance of the baseline design.

The designs were then analyzed in FAST/AeroDyn with a "static" analysis, a simple windspeed sweep, as well as a dynamic load case, the standard "extreme gust with direction change" design load case. The "static" results from the windsweep analysis for the baseline and optimized designs are shown in Figs. 16 – 17. The dynamic analysis wind profile is shown in Fig. 18 and the performance is shown in Figs. 19 and 20. These show a general reduction in blade loads for the #1 designs, but a possible increase in loads with the #2 designs. However, the SERR calculations effectively replace these measures when evaluating the damage tolerance of each design, and the higher loads shown in Fig. 14 for DU #2 compared with DU #1 actually corresponded with lower SERRs. Therefore, the increased loads in Fig. 19 of the DU #2 design with respect to the baseline or DU #1 designs do not translate to reduced damage tolerance, and similarly the reduced loads of DU #1 do not translate to increased damage tolerance. Dynamic analysis of the SERRs will be required to obtain a more accurate characterization of the damage tolerance of each design.

CONCLUSIONS

One of the primary barriers to acceptance of wind energy in the US is the reliability of offshore wind systems. This work attempts to increase the reliability for offshore wind turbine blades by introducing operating and design strategies designed to mitigate the effects of damage while continuing to produce power. Two simple derating strategies were evaluated with their potential to increase annual energy output (AEP), compared with shutdown, while reducing the effects of damage in terms of strain energy release rates. These derating strategies utilize available control systems for modern wind turbines, such as the NREL 5 MW representative model, as a "software" change, with no changes to the "hardware" required for implementation.

To demonstrate a damage tolerant design process, a combined aero/structural optimization process was used to produce several candidates for a 100 m blade. The baseline DU series airfoils were compared with a new set of flat-back (FB) airfoils to investigate their potential to introduce damage tolerance. These candidates revealed that a moderate increase in design TSR allows for a reduction in blade weight and increase in AEP, but stress-based as well as SERR-based fatigue considerations place an upper limit on how much the design TSR should be increased. The FB airfoils seemed to perform better than

Table 4: 100 m blade design details, DU series airfoils.

Design	SNL 100-02	DU #1	DU #2
AEP (GWh)	66.7	66.7	67.3
Weight (kg)	59,043	52,765	55,588
Max Chord (m)	7.59	6.58	7.37
Design TSR	7.35	9.55	8.45
ECD Tip Δ (m)	10.97	10.62	11.28
Spar Life (yr)	15.3	1.9	14.7
TE Life (yr)	72	16.9	70.9
Buckling	2.19	2.02	1.92

Table 5: 100 m blade design details, FB airfoils.

Design	SNL 100-02	FB #1	FB #2
AEP (GWh)	66.7	66.7	67.3
Weight (kg)	59,043	52,876	55,375
Max Chord (m)	7.59	6.87	7.11
Design TSR	7.35	9.4	8.4
ECD Tip Δ (m)	10.97	10.47	11.67
Spar Life (yr)	15.3	33.7	8.3
TE Life (yr)	72	130	50
Buckling	2.19	2.63	2.57

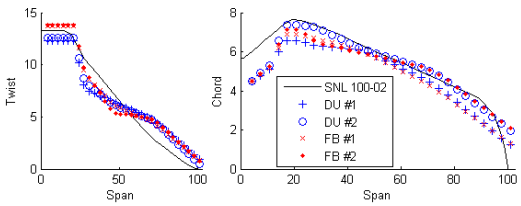

Fig. 11: Chord and twist distributions for two 100 m designs utilizing either DU series or FB airfoils.

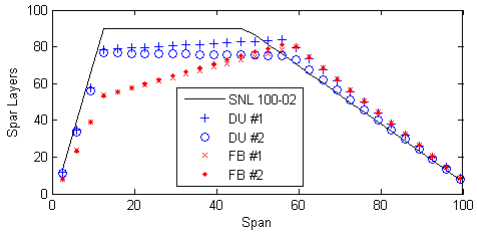

Fig. 12: Spar layer distributions for two 100 m blade designs.

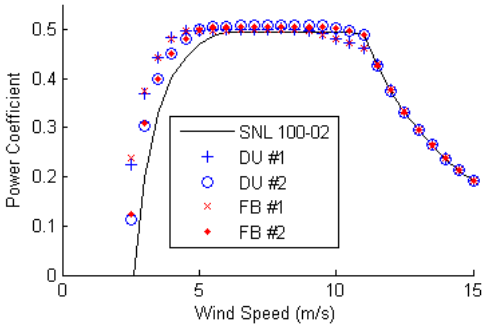

Fig. 13: Predicted power output in terms of Cp from the four different designs.

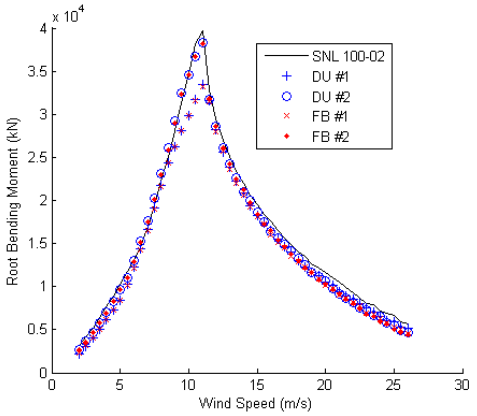

Fig. 14: Root bending moment predictions in kN for 100 m blade designs.

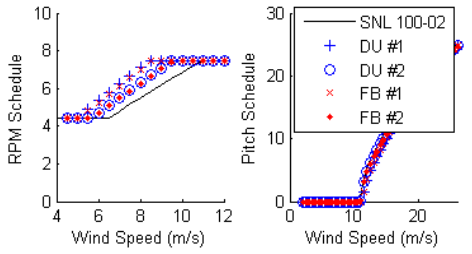

Fig. 15: Design control scheduling for 100 m blade designs. Pitch schedule is nearly identical for the three designs.

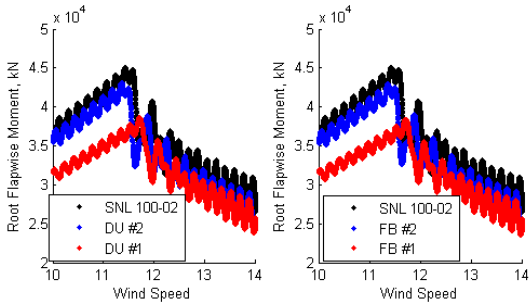

Fig. 16: Flapping moment predictions for 100 m blade designs from windsweep FAST/AeroDyn analysis.

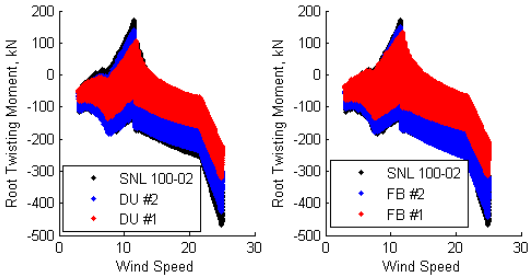

Fig. 17: Twisting moment predictions for 100 m blade designs from windsweep FAST/AeroDyn analysis.

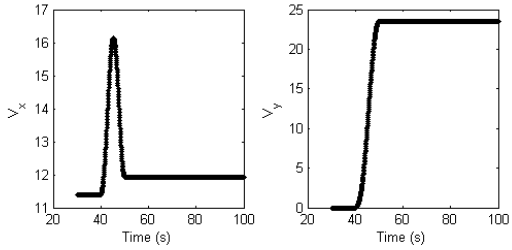

Fig. 18: Wind profile for "extreme coherent gust with direction change" analysis. V_x is aligned with the shaft axis and V_y is perpendicular to the shaft direction (but not vertical).

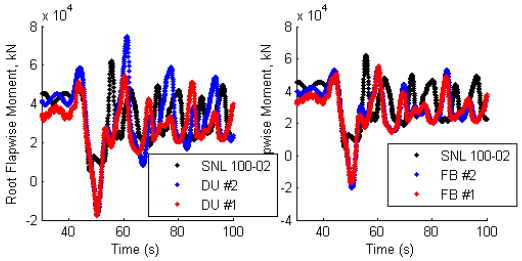

Fig. 19: Root bending moment (kN) time histories from ECD analysis of competing designs.

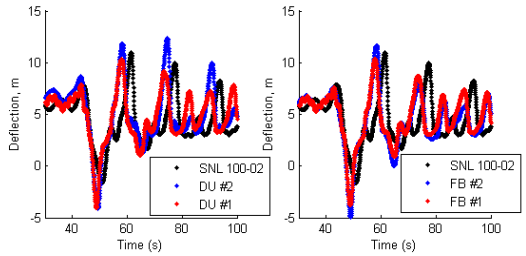

Fig. 20: Tip deflection time histories from "extreme coherent gust with direction change" analysis of competing designs.

the DU airfoils in terms of stress-based fatigue, but generally worse in terms of the trailing edge disbond SERRs. However, the SERRs were lower for the FB airfoils over the 10 – 20 m location, and the flat trailing edge is an ideal location for additional reinforcement. If trailing edge reinforcement can be used to mitigate the SERR results for the FB #1 design, it would satisfy all design requirements and would be a good candidate for a new 100 m FB design.

This study is part of a continuing effort to explore damage tolerant operations and design strategies. The next step in this process will be to refine the accuracy of the SERR results as well as consider other types of common damage, such as a spar/skin disbond. Dynamic analysis of the SERR results will give a more accurate characterization of the damage tolerance of each design. Also, more advanced control strategies may be more effective in reducing the SERRs, especially in dynamic events like the "extreme gust with direction change" load case.

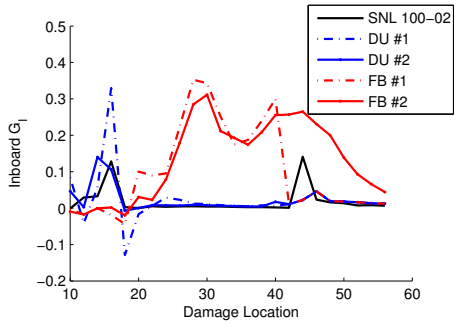

Fig. 21: Inboard G_I comparative measures for 100 m blade designs.

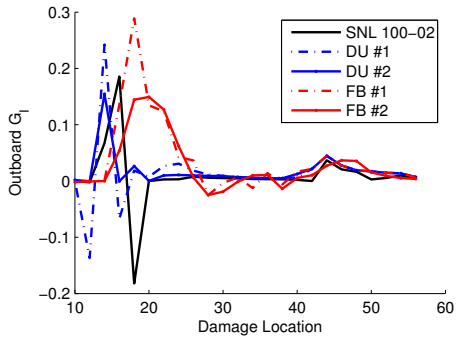

Fig. 22: Outboard G_I comparative measures for 100 m blade designs.

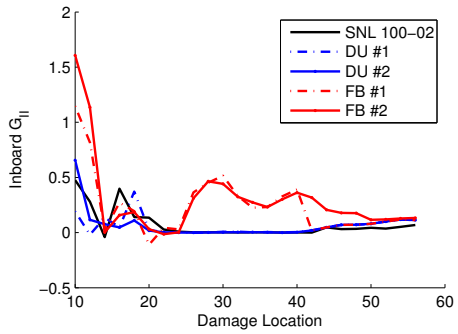

Fig. 23: Inboard G_{II} comparative measures for 100 m blade designs.

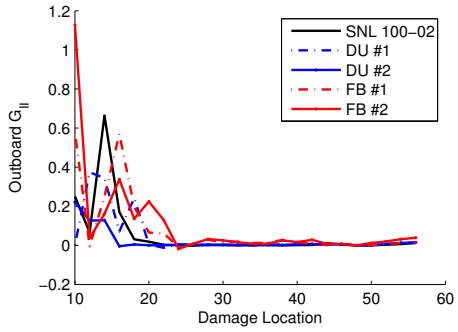

Fig. 24: Outboard G_{II} comparative measures for 100 m blade designs.

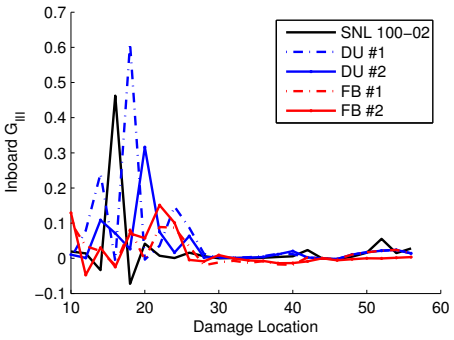

Fig. 25: Inboard G_{III} comparative measures for 100 m blade designs.

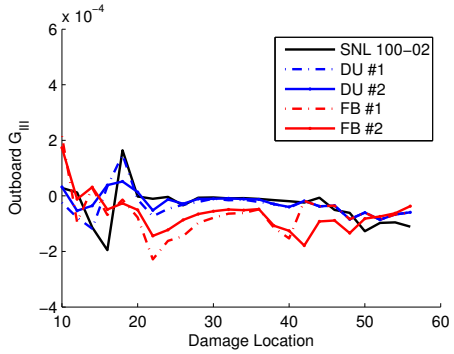

Fig. 26: Outboard G_{III} comparative measures for 100 m blade designs.

REFERENCES

[1]Griffith, D. and Ashwill, T., "The Sandia 100-meter All-glass Baseline Wind Turbine Blade: SNL100-00." Technical Report SAND2011-3779, Sandia National Laboratories, 2011.

[2]Griffith, D., "The SNL100-01 Blade: Carbon Design Studies for the Sandia 100-meter Blade." Technical Report SAND2013-1178, Sandia National Laboratories, 2013.

[3]Griffith, D. T., Resor, B. R., and Ashwill, T. D., "Challenges and Opportunities in Large Offshore Rotor Development: Sandia 100-meter Blade Research," AWEA WINDPOWER 2012 Conference and Exhibition. Atlanta, GA, USA, 2012.

[4]Jonkman, J., Butterfield, S., Musial, W., and Scott, G., "Definition of a 5-MW Reference Wind Turbine for Offshore System Development." Technical Report NREL/TP-500-38060, 2009.

[5]Griffith, D. T., Yoder, N., Resor, B., White, J., and Paquette, J., "Structural Health and Prognostics Management for Offshore Wind Turbines: An Initial Roadmap," Technical Report SAND2012-10109, Sandia National Laboratories, 2012.

[6]Myrent, N., Kusnick, J., Barrett, N., Adams, D., and Griffith, D., "Structural Health and Prognostics Management for Offshore Wind Turbines: Case Studies of Rotor Fault and Blade Damage with Initial OM Cost Modeling," Technical Report SAND2013-2735, Sandia National Laboratories, 2013.

[7]Myrent, N. J., Adams, D. E., and Griffith, D. T., "Aerodynamic Sensitivity Analysis of Rotor Imbalance and Shear Web Disbond Detection Strategies for Offshore Structural Health Prognostics Management of Wind Turbine Blades," 32nd ASME Wind Energy Symposium. National Harbor, Maryland, 2014.

[8]Snyder, B. and Kaiser, M. J., "Ecological and Economic Cost-benefit Analysis of Offshore Wind Energy," *Renewable Energy*, Vol. 34, (6), 2009, pp. 1567–1578.

[9]Frangopol, D. M., Saydam, D., and Kim, S., "Maintenance, Management, Life-cycle Design and Performance of Structures and Infrastructures: a Brief Review," *Structure and Infrastructure Engineering*, Vol. 8, (1), 2012, pp. 1–25.

[10]Rangel-Ramirez, J. G. and Sorensen, J. D., "Risk-based Inspection Planning Optimisation of Offshore Wind Turbines," *Structure and Infrastructure Engineering*, Vol. 8, (5), 2012, pp. 473–481.

[11]Zhang, J., Chowdhury, S., Zhang, J., Tong, W., and Messac, A., "Optimal Preventive Maintenance Time Windows for Offshore Wind Farms Subject to Wake Losses," 12th AIAA Aviation Technology, Integration, and Operations (ATIO) Conference and 14th AIAA/ISSM. Indianapolis, Indiana, 2012.

[12]Wenjin, Z., Fouladirad, M., Berenguer, C., *et al.*, "A Predictive Maintenance Policy Based on the Blade of Offshore Wind Turbine," Annual Reliability and Maintainability Symposium-RAMS 2013, 2013.

[13]Marden, J. R., Ruben, S. D., and Pao, L. Y., "Surveying Game Theoretic Approaches for Wind Farm Optimization," Proceedings of the 50th AIAA Aerospace Sciences Meeting, Nashville, TN., 2012.

[14]Gonzalez, J. S., Payan, M. B., and Santos, J. R., "Optimal Control of Wind Turbines for Minimizing Overall Wake Effect Losses in Offshore Wind Farms," Eurocon, 2013 IEEE, 2013.

[15]Kusiak, A. and Song, Z., "Design of Wind Farm Layout for Maximum Wind Energy Capture," *Renewable Energy*, Vol. 35, (3), 2010, pp. 685–694.

[16]Bossanyi, E., "Further Load Reductions with Individual Pitch Control," *Wind Energy*, Vol. 8, (4), 2005, pp. 481–485.

[17]Xiao, S., Yang, G., and Geng, H., "Individual Pitch Control Design of Wind Turbines for Load Reduction using Sliding Mode Method." ECCE Asia Downunder (ECCE Asia), 2013 IEEE, 2013.

[18]Wang, L., Wang, B., Song, Y., and Zeng, Q., "Fatigue Loads Alleviation of Floating Offshore Wind Turbine Using Individual Pitch Control," *Advances in Vibration Engineering*, Vol. 12, (4), 2013, pp. 377–390.

[19]Larsen, T. J. and Hanson, T. D., "A Method to Avoid Negative Damped Low Frequent Tower Vibrations for a Floating, Pitch Controlled Wind Turbine," *Journal of Physics: Conference Series*, Vol. 75, (1), 2007.

[20]Jonkman, J. M., "Influence of Control on the Pitch Damping of a Floating Wind Turbine," 2008 ASME Wind Energy Symposium, Reno, Nevada., 2008.

[21]Christiansen, S., Bak, T., and Knudsen, T., "Damping Wind and Wave Loads on a Floating Wind Turbine," *IEEE Transactions on Control Systems Technology*, Vol. 6, (8), 2013, pp. 4097–4016.

[22]Namik, H. and Stol, K., "Individual Blade Pitch Control of Floating Offshore Wind Turbines," *Wind Energy*, Vol. 13, (1), 2010, pp. 74–85.

[23]Rotea, M., Lackner, M., and Saheba, R., "Active Structural Control of Offshore Wind Turbines," 48th AIAA Aerospace Sciences Meeting and Exhibit, Orlando, Florida, 2010.

[24]Yamashita, A. and Sekita, K., "Analysis of the Fatigue Damage on the Large Scale Offshore Wind Turbines Exposed to Wind and Wave Loads," Proceeding of the 14th International Offshore and Polar Engineering Conference, 2004.

[25]Trumars, J. M., Tarp-Johansen, N. J., and Krogh, T., "Fatigue Loads on Offshore Wind Turbines due to Weakly Non-Linear Waves," 24th International Conference on Offshore Mechanics and Arctic Engineering, 2005.

[26]Frost, S. A., Goebel, K., Balas, M. J., and Henderson, M. T., "Integrating Systems Health Management with Adaptive Contingency Control for Wind Turbines," 51st AIAA Aerospace Sciences Meeting Including the New Horizons Forum and Aerospace Exposition. Grapevine, TX, USA, 2013.

[27]Fan, X., Sun, Q., and Kikuchi, M., "Review of Damage Tolerant Analysis of Laminated Composites," *Journal of Solid Mechanics Vol*, Vol. 2, (3), 2010, pp. 275–289.

[28]Sutherland, H., "On the Fatigue Analysis of Wind Turbines," Technical Report SAND99-0089, Sandia National Laboratories, 1999.

[29]Sutherland, H. and Mandell, J., "Effect of Mean Stress on the Damage of Wind Turbine Blades." 2004 ASME Wind Energy Symposium, AIAA/ASME., 2004.

[30]Mandell, J., Samborsky, J., Wahl, D., and Sutherland, N., "Effect of Mean Stress on the Damage of Wind Turbine Blades." International Committee on Composite Materials Conference 14, San Diego, CA., 2003.

[31]Krueger, R., "Virtual Crack Closure Technique: History, Approach, and Applications." *Applied Mechanics Review*, Vol. 57, (2), 2004.

[32]Eder, M., Bitsche, R., Nielsen, M., and Branner, K., "A Practical Approach to Fracture Analysis at the Trailing Edge of Wind Turbine Rotor Blades." *Wind Energy*, Vol. 17, (3), 2013.

[33]Lopes, C., Seresta, O., Abdalla, M., Gürdal, Z., Thuis, B., and Camanho, P., "Stacking sequence dispersion and tow-placement for improved damage tolerance," Proceedings of the 49th Structures, Structural Dynamics, and Materials Conference, Schaumburg, Illinois, Paper AIAA 2008-1735, April 7 – 10, 2008.

[34]Kim, H., Kwon, H., and Keune, J., "Buckling Initiation and Disbond Growth in Adhesively Bonded Composite Flanges." 44th AIAA/ASME/ASCE/AHS/ASC Structures, Structural Dynamics, and Materials Conference. Norfolk, VA., 2003.

[35]Schaumann, P. and Wilke, F., "Enhanced Structural Design for Offshore Wind Turbines," XICAT 2006, Xi'an International Conference of Architecture and Technology, 2006.

[36]Wetzel, K., "Defect-Tolerant Structural Design of Wind Turbine Blades." 50th AIAA/ASME/ASCE/AHS/ASC Structures, Structural Dynamics, and Materials Conference. Palm Beach, FL., 2009.

[37]Berg, J. C. and Resor, B. R., "Numerical Manufacturing And Design Tool (NuMAD v2.0) for Wind Turbine Blades: User's Guide," Technical Report SAND2012-7028, Sandia National Laboratories, 2012.

[38]Berg, J., Paquette, J., and Resor, B., "Mapping of 1D Beam Loads to the 3D Wind Blade for Buckling Analysis," 52nd AIAA/ASME/ASCE/AHS/ASC Structures, Structural Dynamics, and Materials Conference. Denver, Colorado, 2011.

[39]Pryor, S., Nielson, M., Barthelmie, R., and Mann, J., "Can Satellite Sampling of Offshore Wind Speeds Realistically Represent Wind Speed Distributions? Part II: Quantifying Uncertainties Associated with Distribution Fitting Methods." *American Meteorological Society*, Vol. 43, (5), May 2004, pp. 739–750.

[40]Palutikof, J., Halliday, J., Watson, G., Holt, T., Barthelmie, R., Coelingh, J., Folkerts, L., and Cleijne, J., "Predicting the Wind Energy resource in the Offshore seas of Europe," Symposium on Environmental Applications; American Meteorological Society 82.

[41]Sale, D., "HARP Opt, Horizontal Axis Rotor Performance Optimization," National Renewable Energy Laboratory. http://wind.nrel.gov/designcodes/simulators/HARP_Opt/, Accessed: July 2013.

[42]"Numerical Manufacturing And Design Tool (NuMAD)," Sandia National Laboratories. http://energy.sandia.gov/?page_id=2238, Accessed: July 2013.

[43]Sale, D., "CoBlade, Open Source Software for Composite Wind Turbine Blades," https://code.google.com/p/co-blade/, Accessed: July 2013.